OpenParEM3D

Electromagnetic Simulator

Brian Young

January 9, 2024

Agenda

- Motivation
- Features
- S-parameters
- 3D FEM setup
- Adaptive mesh refinement
- Examples and discussion
- Regression suites
- Conclusion

Motivation

- Lack of a free or very low-cost frequency-domain S-parameter electromagnetic simulator inhibits exploration of new ideas and development of new products
- Target audience
  - Engineers wanting to explore ideas at home
  - Continuing education
  - Students
  - Small startups
- Feasibility
  - Leverage existing open-source projects
  - CAD (FreeCAD), meshing (gmsh), FEM (MFEM), visualization (ParaView)
  - “Just” need to glue it all together

Features

- Full-wave time-harmonic 3D electromagnetic simulator
- Computing
  - Electric and magnetic fields
  - S-parameters between 2D ports on the surface of the 3D space
- Arbitrary high-order elements
  - courtesy of MFEM, ParaView [up to 6^{th} order]
- Parallel processing via MPI
  - courtesy of MFEM, PETSc, and SLEPc plus custom code
- Adaptive mesh refinement
  - courtesy of MFEM plus custom code
- TBD: impedance boundary condition for conductor losses and antennas

S-parameters

- “S-parameters” is short for “scattering parameters”
  - Links incident and reflected waves at the ports of a 3D volume
- Dominant in engineering to include electromagnetic results in circuit simulations and for performance analyses
- A “must have” output for a practical simulator

S-parameter Matrix Extraction

Propagating waves are modes on transmission lines or waveguides feeding N ports.

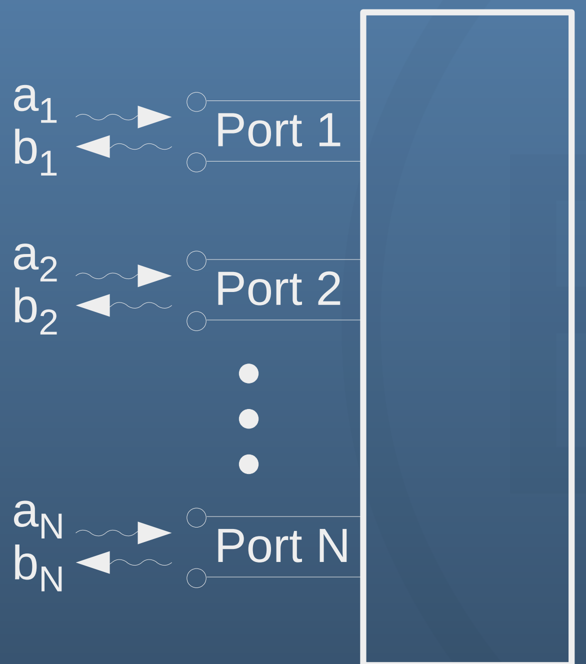

a_i is the incident wave to port i

b_i is the reflected wave from port i

S-parameter matrix

$$\begin{bmatrix} b_1 \\ b_2 \\ \vdots \\ b_N \end{bmatrix} = \begin{bmatrix} S_{11} & S_{12} & \cdots & S_{1N} \\ S_{21} & S_{22} & \cdots & S_{2N} \\ \vdots & \vdots & \ddots & \vdots \\ S_{N1} & S_{N2} & \cdots & S_{NN} \end{bmatrix} \begin{bmatrix} a_1 \\ a_2 \\ \vdots \\ a_N \end{bmatrix}$$

- Define ports - 2D (flat) on surface of 3D space
- Solve 1 column at a time
  - Drive port i such that $a_i \neq 0$
  - Apply absorbing boundary condition on all other ports, then $a_k = 0$ for $k \neq i$
- Solve the 3D problem N times for i=1,..,N
- Separate a_i and b_i at the driven port
- Output frequency-dependent S-parameters in Touchstone file format

Driving a_i

Port i: 2D simulation for fields, α, β, Z_o

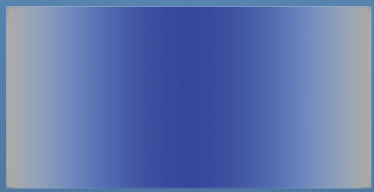

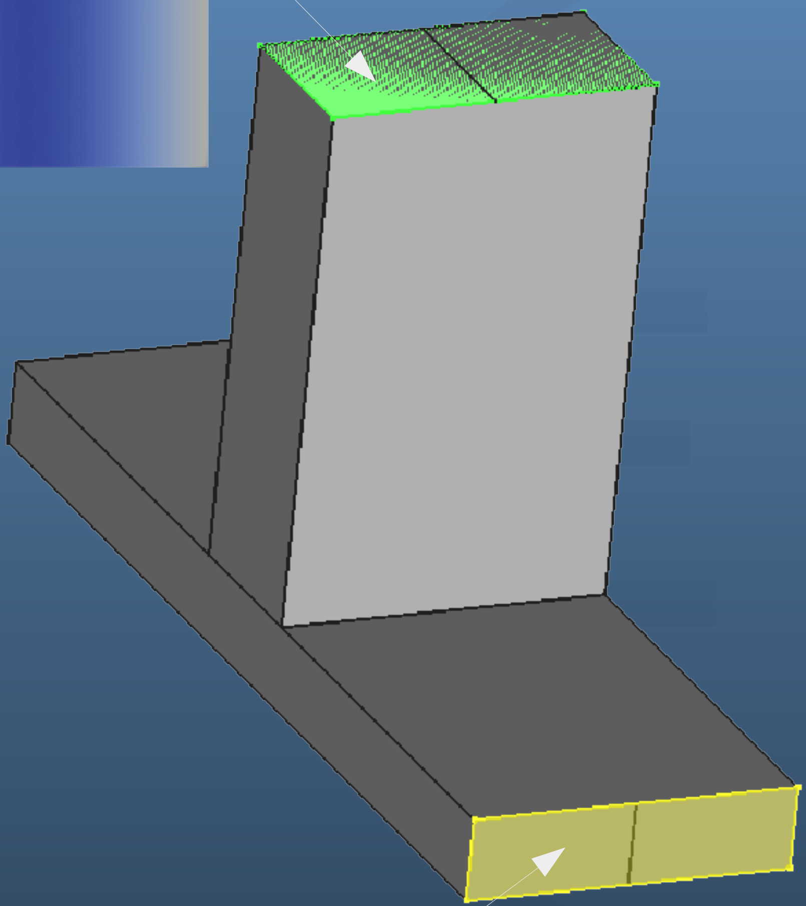

Port k: absorbing boundary

- MFEM's ParSubMesh functionality is used to extract 2D meshes
- A 2D simulation is run for each port with OpenParEM2D*
- The 2D field solution for port i is applied to the 3D space, forcing the 3D fields at the port to take the 2D configuration
- An absorbing boundary condition is applied at the other ports
- 3D electromagnetic simulation is run
- Repeat for each port
- Extract S-paramters (more later)

* OpenParEM2D was presented at the 2022 MFEM Community Workshop.

3D FEM Setup

- Weak form of the wave equation in $\overline{E}$

$$\iiint_{\Omega} \frac{1}{\mu_r} \nabla \times \overline{E} \cdot \nabla \times \overline{W}\, dV - k_0^2 \iiint_{\Omega} \epsilon_r \overline{E} \cdot \overline{W}\, dV + \iint_{S} \frac{1}{\mu_r} \hat{n} \times \nabla \times \overline{E} \cdot \overline{W}\, dS = 0$$

MFEM CurlCurlIntegrator

MFEM VectorFEMassIntegrator

Surface of the 3D space

- Separate the surface integral

$$\iint_{S} \frac{1}{\mu_r} \hat{n} \times \nabla \times \overline{E} \cdot \overline{W}\, dS = \iint_{S_b} \frac{1}{\mu_r} \hat{n} \times \nabla \times \overline{E} \cdot \overline{W}\, dS + \sum_{i=1}^{N} \iint_{S_{pi}} \frac{1}{\mu_r} \hat{n} \times \nabla \times \overline{E} \cdot \overline{W}\, dS$$

PEC and/or PMC boundary
Apply BC directly to the matrix
[DOF=0 for PEC, keep DOF for PMC]

N ports

2D Port Setup on Surface

- Setup of the surface integral (from prior slide)

$$\iint_S \frac{1}{\mu_r} \hat{n} \times \nabla \times \overline{E} \cdot \overline{W}\, dS = \iint_{S_b} \frac{1}{\mu_r} \hat{n} \times \nabla \times \overline{E} \cdot \overline{W}\, dS + \sum_{i=1}^{N} \iint_{S_{pi}} \frac{1}{\mu_r} \hat{n} \times \nabla \times \overline{E} \cdot \overline{W}\, dS$$

DOF manipulation — Not Supported in MFEM

- Apply a propagating assumption at the ports
  - A first-order absorbing boundary condition

$$\hat{n} \times \nabla \times \overline{E} = -\frac{\partial \overline{E}_t}{\partial n} + \nabla_t E_n \quad \leftarrow \text{Identity}$$

$$= \gamma \overline{E}_t + \nabla_t E_n \quad \leftarrow \text{Propagation Assumption}$$

$$\frac{\partial \overline{E}_t}{\partial n} = \frac{\partial \overline{E}(t) \mathrm{e}_t^{-\gamma n}}{\partial n} = -\gamma \overline{E}(t)$$

$\gamma \overline{E}_t$: MFEM VectorFEMassIntegrator

$\nabla_t E_n$: Not supported in MFEM for Nedelec elements
- Normal component on the boundary
- Assume that this term is negligible

On the Neglected Gradient Term

- On the port boundaries, the gradient term of the normal component is neglected
- A zero gradient of a non-zero E_n is not physically realizable
  - This means that it is assumed that $E_n=0$
- The implemented boundary condition strictly only applies to transverse electric modes (TE and TEM)
  - TE and TEM cases dominate problems of interest. These include microstrip, stripline, coax, triax, slot line, coplanar waveguide, the TE10 mode in rectangular waveguide, and generally, any N-conductor transmission line
  - <u>So the TE restriction in practice is not significantly limiting</u>
- Non-TE modes suffer field distortion at the port leading to a reflection
- Non-TE modes at the boundaries can be supported by using TE modes at the ports with 3D transitions to the required non-TE ports followed by de-embedding (like lab measurements)
- For quasi- TE and TEM modes, E_n is small compared to $\overline{\overline{E}}_t$
  - The error caused by the reflection is determined by the strength of E_n
  - For quasi- TE and TEM modes, the reduction in accuracy may be acceptable
- Future work is needed to relax this restriction, for example, by including the gradient term or by implementing a perfectly matched layer (PML) boundary condition

Top-Level Implementation Details

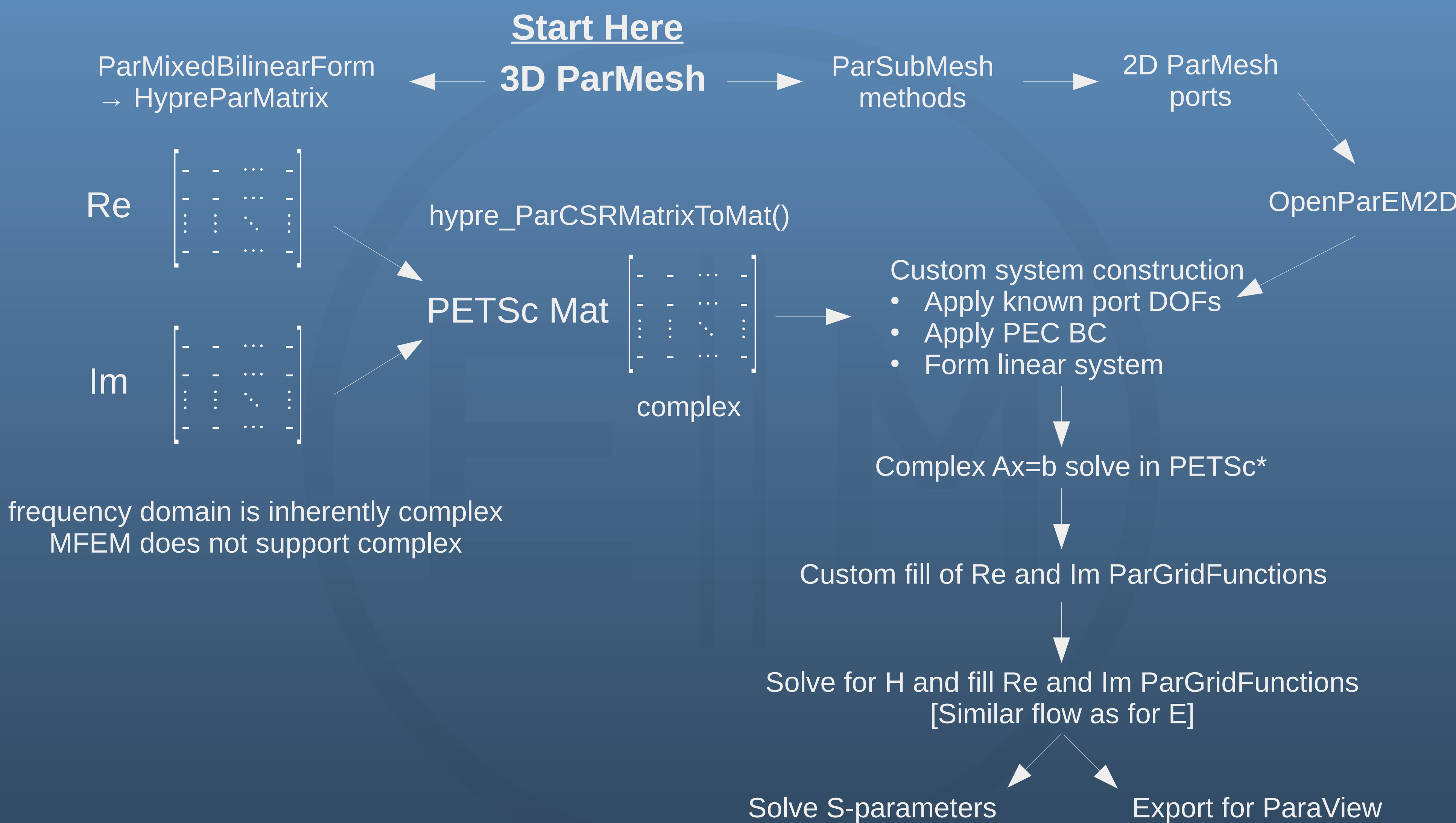

* A real formulation was tried in MFEM, but poor convergence was observed. For background, see David Day and Mike Heroux, “Solving Complex-valued Linear Systems via Equivalent Real Formulations”, report from Sandia National Laboratories, May 9, 2000. There is a later SIAM paper based on this work.

S_{ii}: Separating a_i and b_i

- At this point, the 3D fields for $\overline{E}$ and $\overline{H}$ are computed.
  - The E-field from the 2D port simulation was applied at port i [i.e. the driving port]
  - Cannot differentiate $\overline{E}^{+}$ from $\overline{E}^{-}$ just from the port i E-field.
  - Requires $\overline{H}$ to separate the two
- Just use the tangential components since they dominate in practical applications

At Port i, the Driving Port

$$\overline{E}_{ti}=C_{1i}\overline{E}^{+}_{ti}+C_{2i}\overline{E}^{-}_{ti}$$ ← Split with weights

$$\iint_{S_i}\overline{E}^{-*}_{ti}\cdot\overline{E}_{ti}\,dS=C_{1i}\iint_{S_i}\overline{E}^{-*}_{ti}\cdot\overline{E}^{+}_{ti}\,dS+C_{2i}\iint_{S_i}\overline{E}^{-*}_{ti}\cdot\overline{E}^{-}_{ti}\,dS$$ ← Inner products supported by MFEM

$$\overline{E}^{-}_{ti}=\overline{E}^{+}_{ti}$$

$$\iint_{S_i}\overline{E}^{+*}_{ti}\cdot\overline{E}_{ti}\,dS=C_{1i}\iint_{S_i}\overline{E}^{+*}_{ti}\cdot\overline{E}^{+}_{ti}\,dS+C_{2i}\iint_{S_i}\overline{E}^{+*}_{ti}\cdot\overline{E}^{+}_{ti}\,dS$$ → $$e_{0i}=\left(C_{1i}+C_{2i}\right)e_{2i}$$

$$C_{1i}=\frac{1}{2}\left(\frac{e_{0i}}{e_{2i}}+\frac{h_{0i}}{h_{2i}}\right)$$

$$C_{2i}=\frac{1}{2}\left(\frac{e_{0i}}{e_{2i}}-\frac{h_{0i}}{h_{2i}}\right)$$

$$\overline{H}_{ti}=C_{1i}\overline{H}^{+}_{ti}+C_{2i}\overline{H}^{-}_{ti}$$ ← Same mode, same weights

$$\iint_{S_i}\overline{H}^{-*}_{ti}\cdot\overline{H}_{ti}\,dS=C_{1i}\iint_{S_i}\overline{H}^{-*}_{ti}\cdot\overline{H}^{+}_{ti}\,dS+C_{2i}\iint_{S_i}\overline{H}^{-*}_{ti}\cdot\overline{H}^{-}_{ti}\,dS$$

$$\overline{H}^{-}_{ti}=-\overline{H}^{+}_{ti}$$ ← Note the change in sign

$$\iint_{S_i}\overline{H}^{+*}_{ti}\cdot\overline{H}_{ti}\,dS=C_{1i}\iint_{S_i}\overline{H}^{+*}_{ti}\cdot\overline{H}^{+}_{ti}\,dS-C_{2i}\iint_{S_i}\overline{H}^{+*}_{ti}\cdot\overline{H}^{+}_{ti}\,dS$$ → $$h_{0i}=\left(C_{1i}-C_{2i}\right)h_{2i}$$

S_{ii}

- $\overline{E}^{+}$ is the +z direction in OpenParEM2D
  - Away from the 3D space, so related to b
  - $\overline{E}^{-}$ is then related to a
- Voltage wave relationships to S: $a_i = \dfrac{V_i^+}{\sqrt{Z_{oi}}}$ $\quad b_i = \dfrac{V_i^-}{\sqrt{Z_{oi}}}$
- Proportional to the weights:

  (field structure is the same) $a_i = \dfrac{C_{2\mathrm{i}}}{\sqrt{Z_{oi}}}$ $\quad b_i = \dfrac{C_{1\mathrm{i}}}{\sqrt{Z_{oi}}}$
- S_{ii}:

$$S_{ii} = \frac{b_i}{a_i} = \left(\frac{e_{0\mathrm{i}}}{e_{2\mathrm{i}}} + \frac{h_{0\mathrm{i}}}{h_{2\mathrm{i}}}\right) \Big/ \left(\frac{e_{0\mathrm{i}}}{e_{2\mathrm{i}}} - \frac{h_{0\mathrm{i}}}{h_{2\mathrm{i}}}\right)$$

S_{ji}

- Use direct calculation with voltages*

Integrate at the output port (no reverse wave): $V_j^+ = V_j$

Integrate at the input port, then take the fraction traveling towards the 3D space: $V_i^- = C_{2i} V_i$

$$S_{ji} = \frac{b_j}{a_i} = \left| \frac{V_j^+}{\sqrt{Z_{oj}}} \right| / \left| \frac{V_i^-}{\sqrt{Z_{oi}}} \right|$$

Use power/voltage definition for Z_o

- S_{ji}:

$$S_{ji} = \frac{b_j}{a_i} = \left| \frac{V_j}{\sqrt{Z_{oj}}} \right| / \left| \frac{C_{2i} V_i}{\sqrt{Z_{oi}}} \right|$$

* Can also use currents, which is a future upgrade, to enable the power/current definition of Z_o.

Adaptive Mesh Refinement (AMR)

- Follows the setup used in the MFEM Tesla miniapp
  - CurlCurlIntegrator on $\overline{E}$, RT elements for flux, and ND elements for smoothed flux
  - Merge errors from both Re($\overline{E}$) and Im($\overline{E}$)
- Extract errors from several solutions
  - Per driven port
  - Combine across all driven ports
  - Apply threshold refinement with a cap on the number of elements to refine
- Refine using ParMesh::GeneralRefinement
- Convergence test is on S. Calculate an error criteria at the Nth iteration
  - error=max column norm $\{\overline{S}_N^{-1}(\overline{S}_N-\overline{S}_{N-1})\}$
- Options for sequential number of iterations that must meet the convergence criteria
- Options for AMR at multiple frequencies
- Issue? Degradation of mesh quality with each iteration, especially at ports

Examples and Discussion

WR90 Loaded Rectangular Waveguide

- Exact solution
  - |S11| in dB → -∞
  - phase shift from high-resolution OpenParEM2D simulation
- High accuracy with regular improvement to a very low noise floor

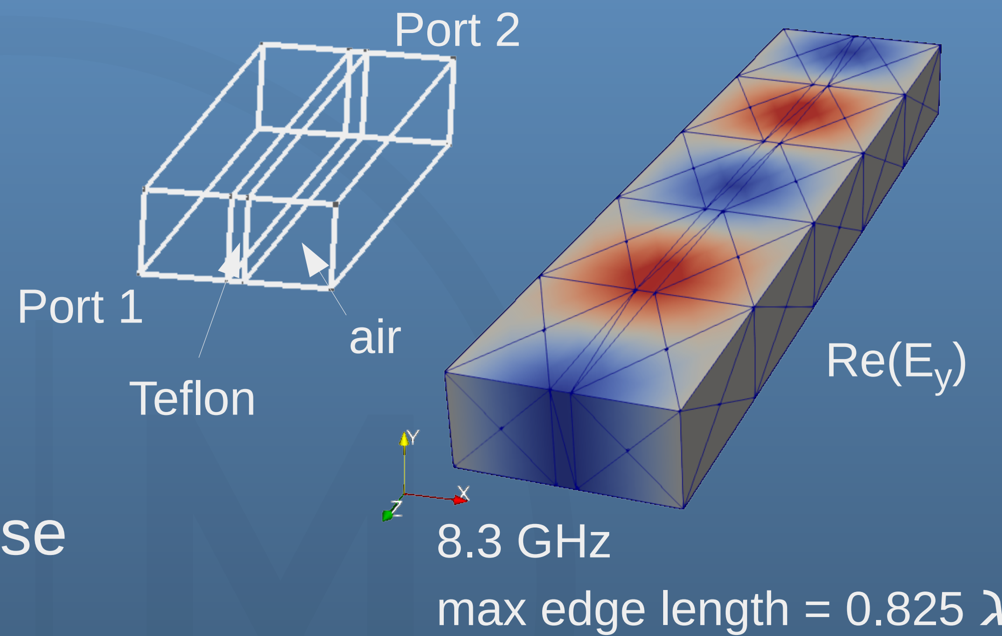

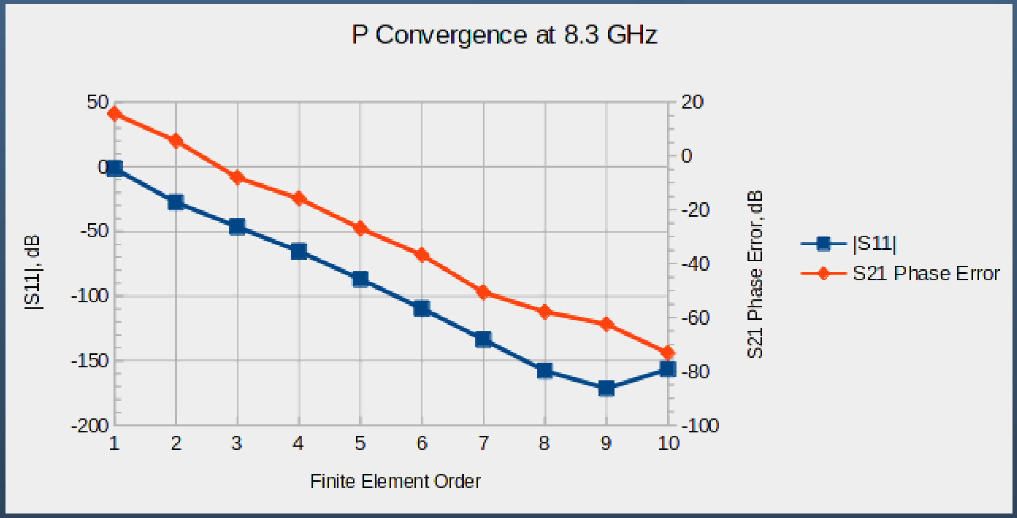

h-Convergence with AMR

- WR90 loaded rectangular waveguide at 8.3 GHz
- Effective AMR
- Accuracy improves with AMR and FEM order
- Favor FEM order over iterations

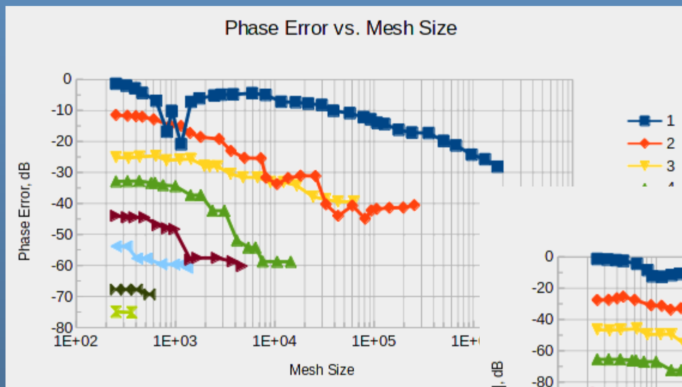

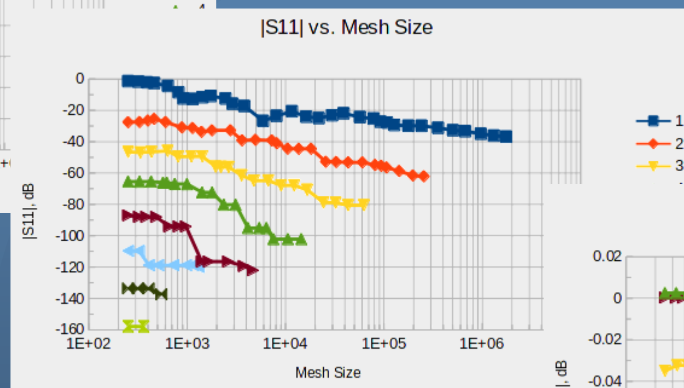

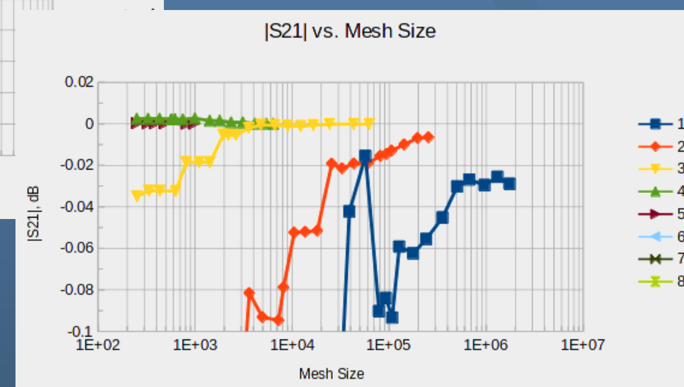

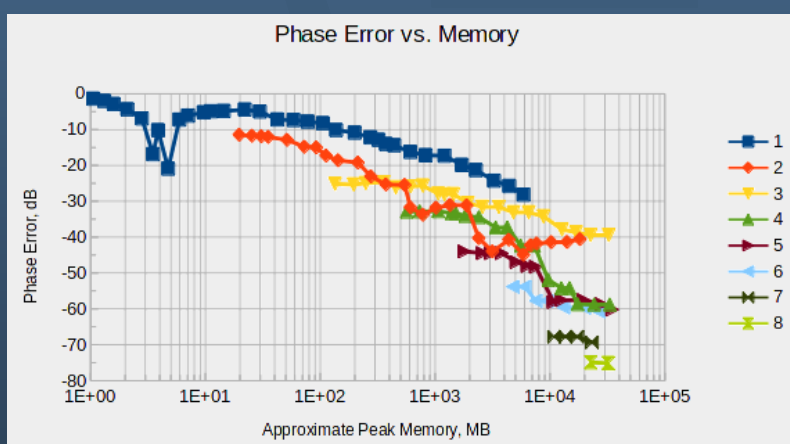

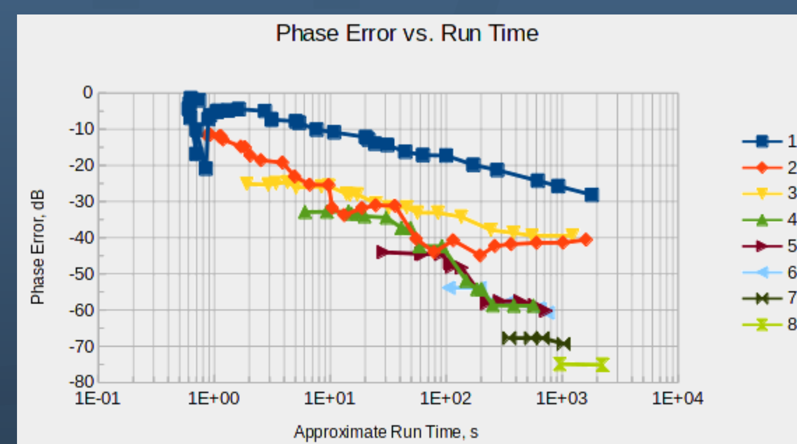

WR75 with Dielectric Puck

- Solve with and without AMR
  - 2^{nd} order, AMR: 575 s
  - 4^{th} order: 968 s
- Excellent agreement between runs with and without AMR
- Excellent agreement between this and prior work

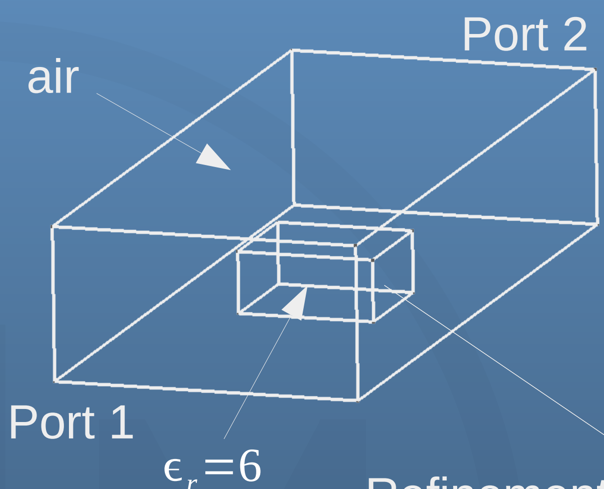

Refinement focussed on the puck

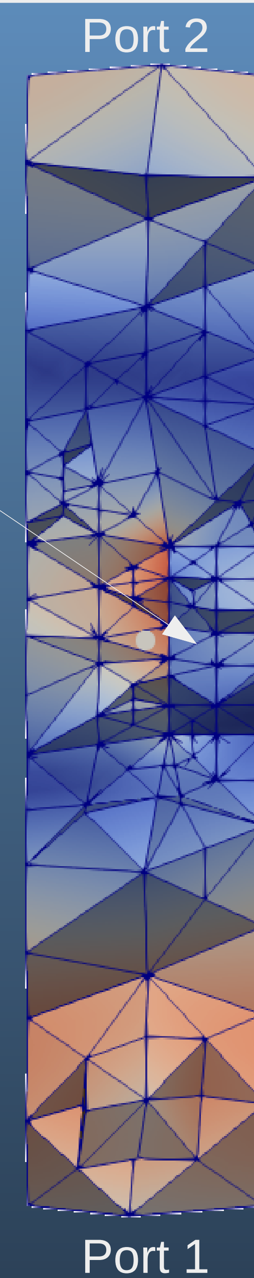

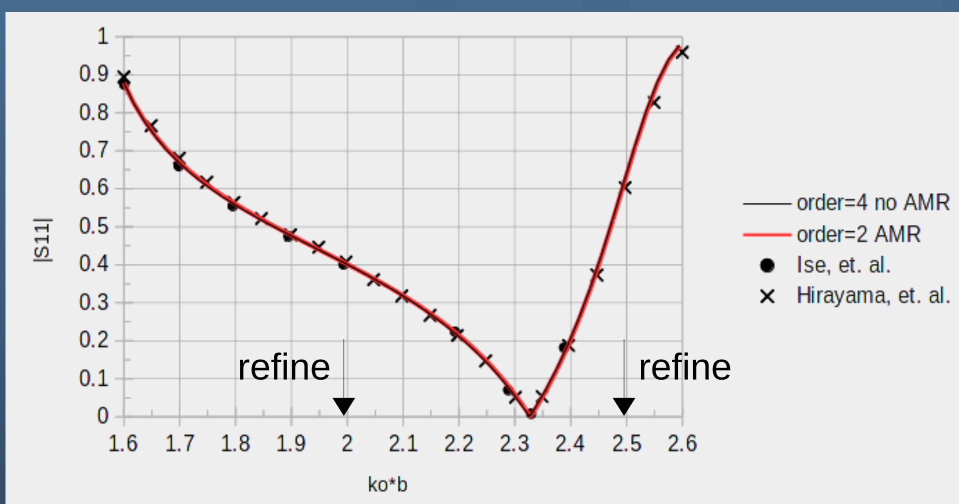

at 10 GHz
No AMR: max edge length = 0.825 ג
AMR: max edge length = 0.230 ג

- K. Ise, K. Inoue, and M. Koshiba, “Three-Dimensional Finite-Element Solution of Dielectric Scattering Obstacles in a Rectangular Waveguide,” *IEEE Trans. Microwave Theory and Techniques*, vol. 38, no. 9, Sept. 1990, pp. 1352-1359.
- K. Hirayama, Md. Alam, Y. Hayashi, and M. Koshiba, “Vector Finite Element Method with Mixed-Interpolation-Type Triangular-Prism Element for Waveguide Discontinuities”, *IEEE Trans. Microwave Theory and Techniques*, vol. 42, no. 12, Dec. 1994, pp. 2311-2316.

WR75 Waveguide T-Junction

- WR75 lossless waveguide splitting to two half-height waveguides for an even power split
- 4th order elements with no adaptive refinement
- Excellent agreement between this work and the referenced paper

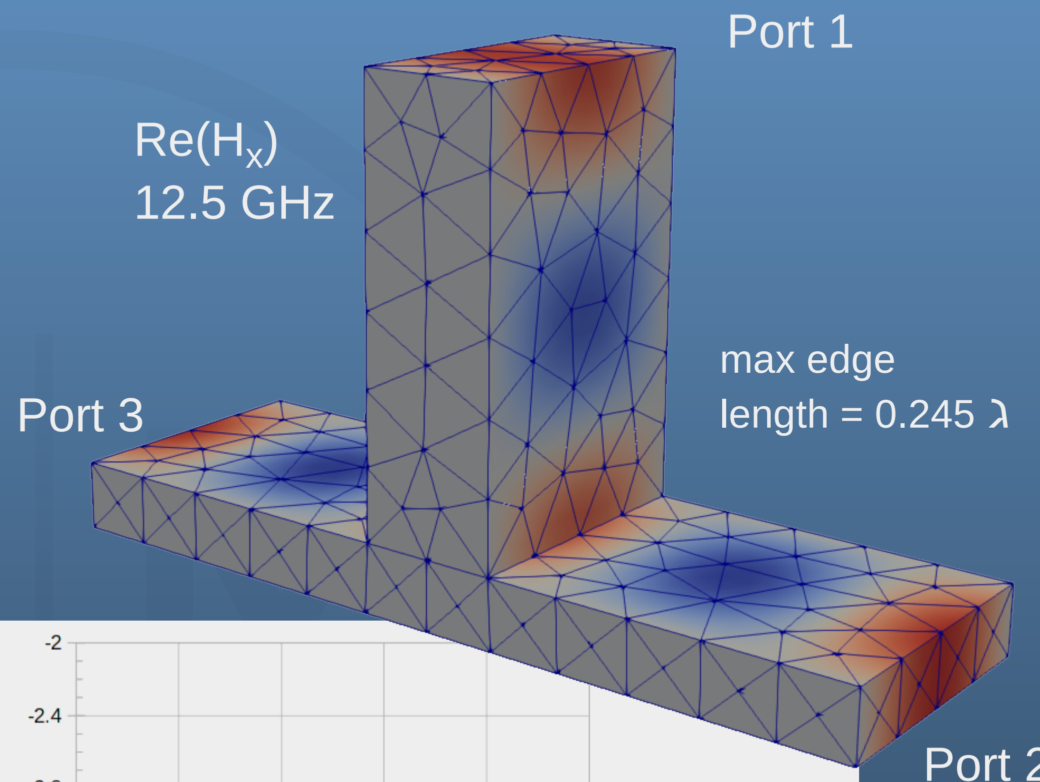

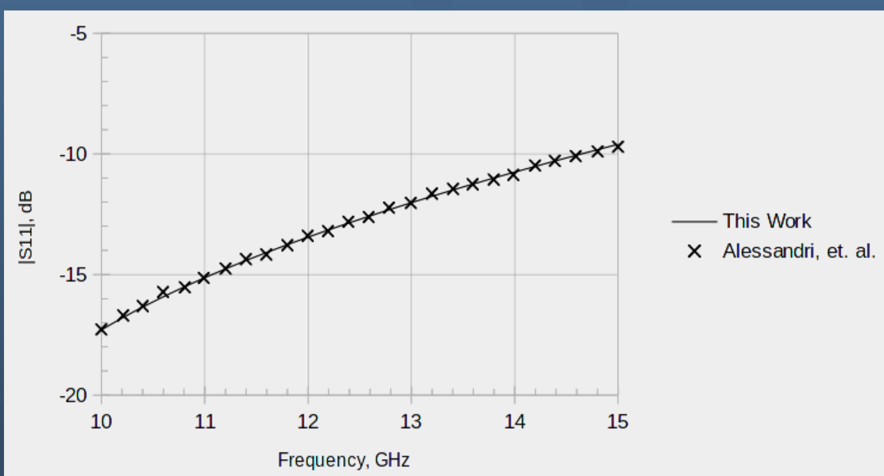

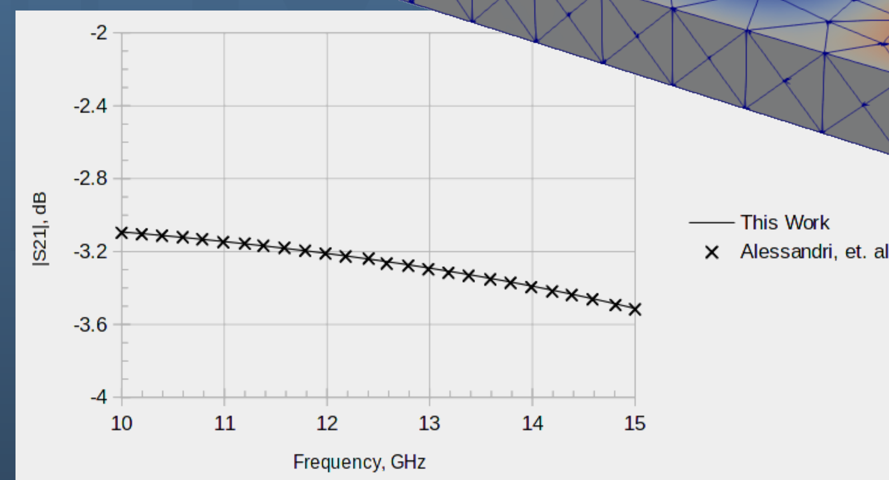

- F. Alessandri, M. Dionigi, and R. Rorrentino, "Rigorous Analysis of Compensated E-plane Junctions in Rectangular Waveguide," *1995 IEEE MTT-S Digest*, pp. 987-990.

Microstrip Bridge

- Microstrip on GaAs bridging across a gap through a block of variable dielectric constant material
- 5th order elements with no adaptive refinement
  - Use the same mesh throughout
- Excellent agreement between this work and the referenced paper

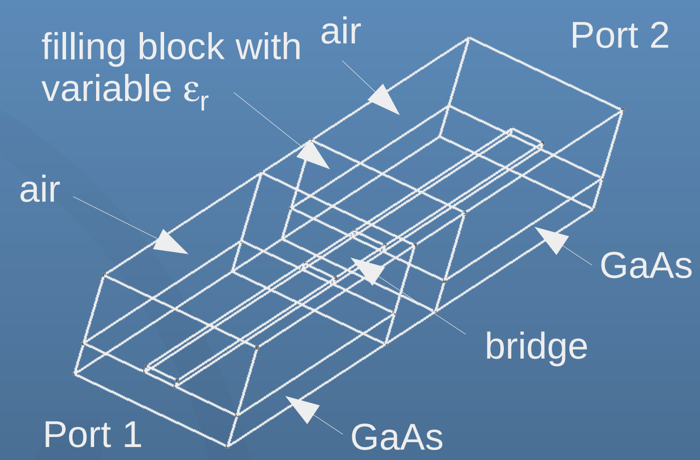

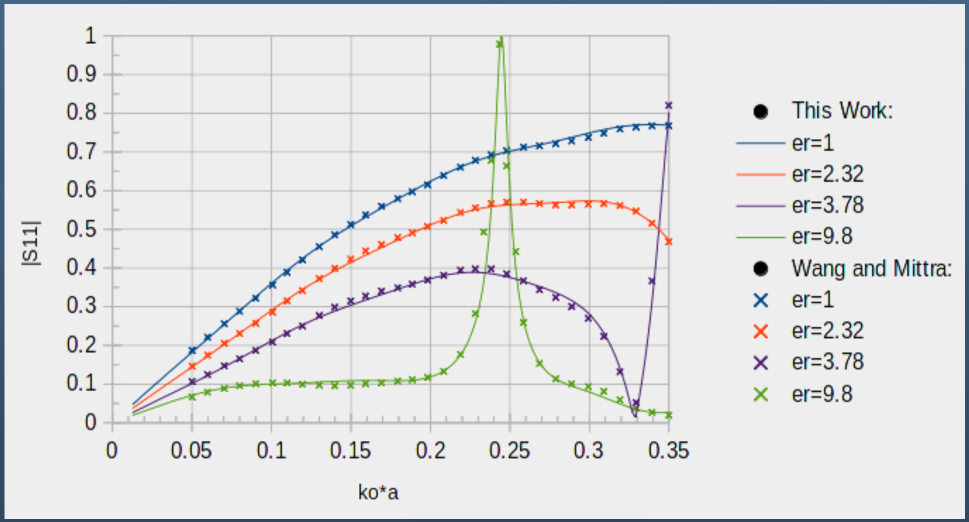

- J.-S. Wang, and R. Mittra, “Finite Element Analysis of MMIC Structures and Electronic Packages Using Absorbing Boundary Conditions,” IEEE. Trans. Microwave Theory and Techniques, vol. 42, no. 3, March 1994, pp. 441-449.

Slotline Step

- ½ slotline on symmetry
- substrate with ε_r=2.22
- 3rd order finite elements with 11 passes of AMR at 35 GHz with 0.001 convergence criteria
- Excellent agreement between this work and the referenced paper

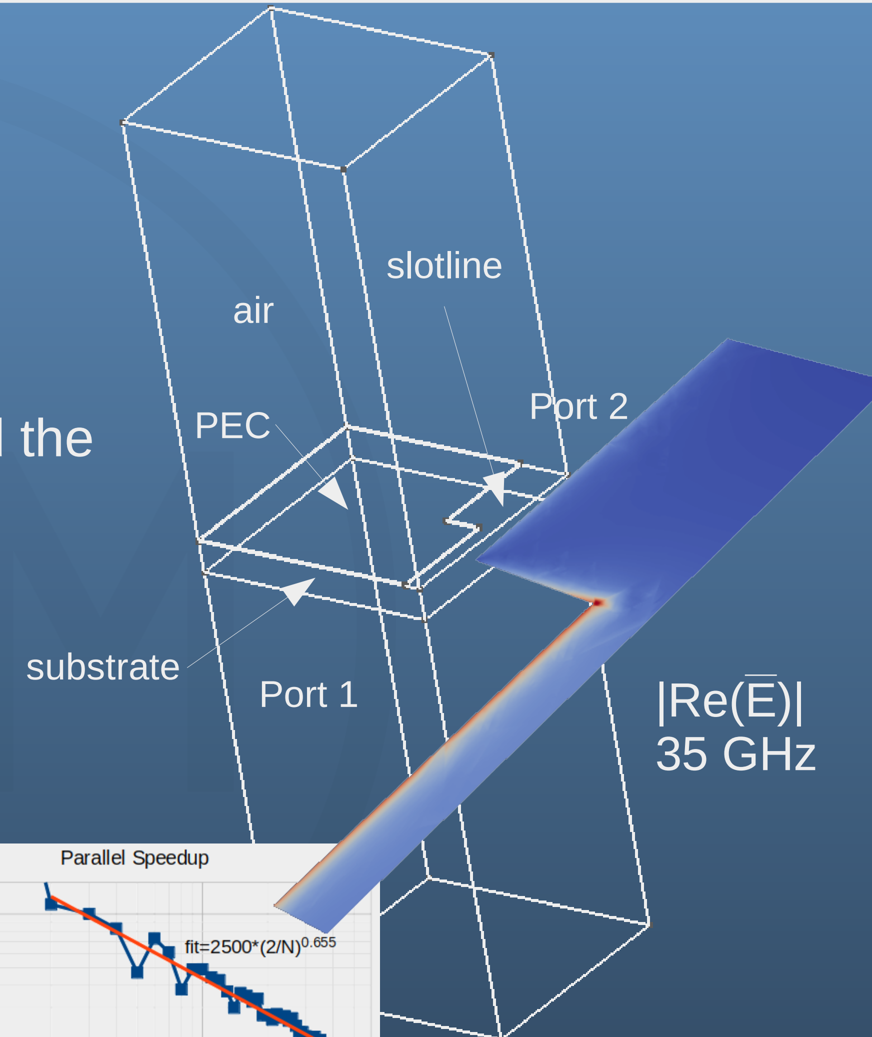

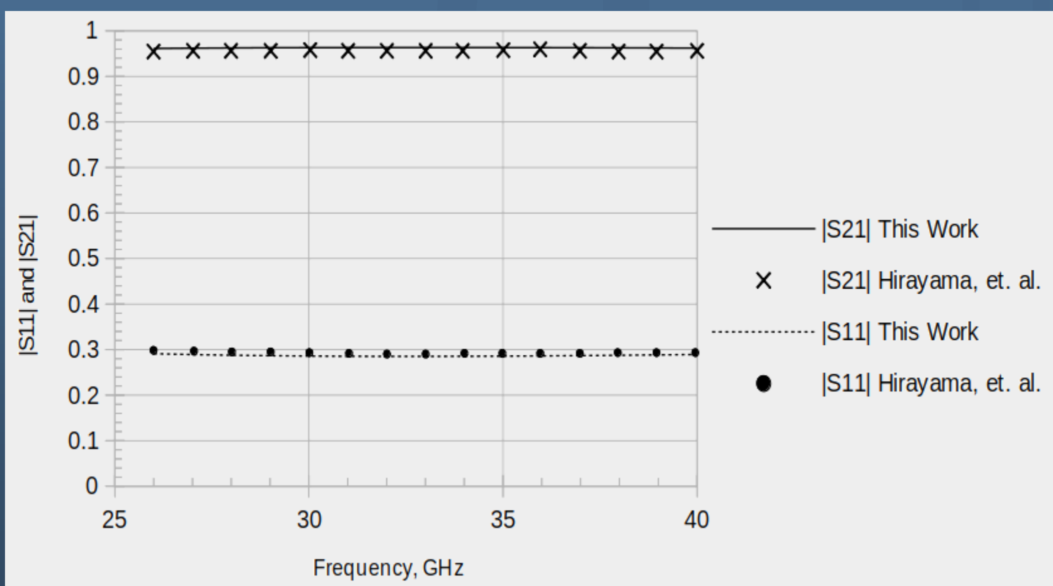

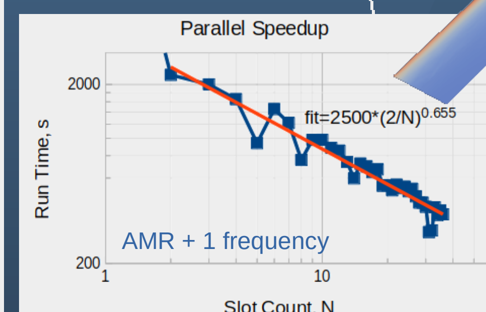

- K. Hirayama, Md. Alam, Y. Hayashi, and M. Koshiba, "Vector Finite Element Method with Mixed-Interpolation-Type Triangular-Prism Element for Waveguide Discontinuities," IEEE Trans. Microwave Theory and Techniques, vol. 42, no. 12, Dec. 1994, pp. 2311-2316.

Microstrip Filter

- Simulation with dielectric losses only
  - conductor losses not yet supported
- 2nd order elements
- AMR with 9 iterations at 4 GHz with 0.02 convergence criteria
- Good agreement considering the differences in losses

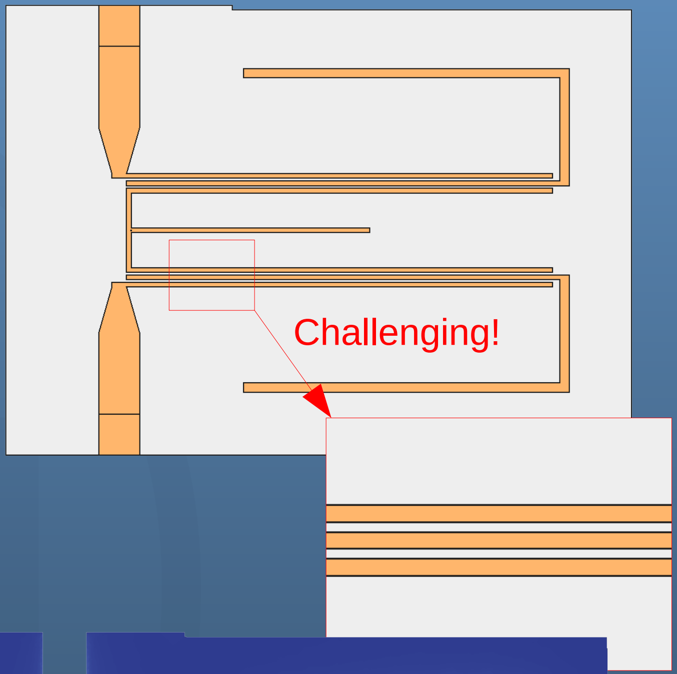

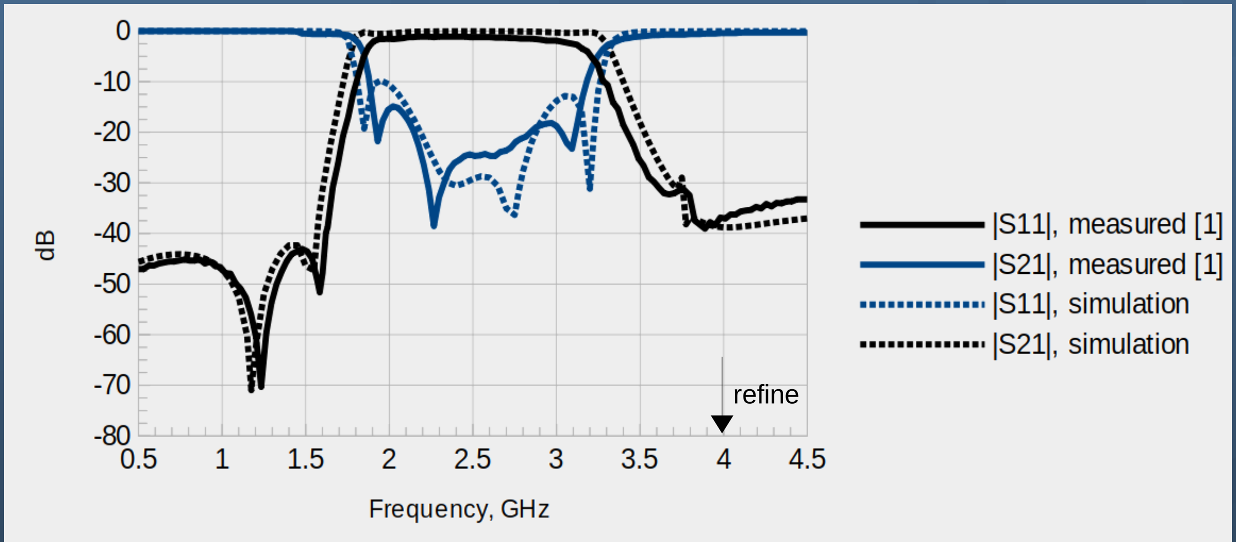

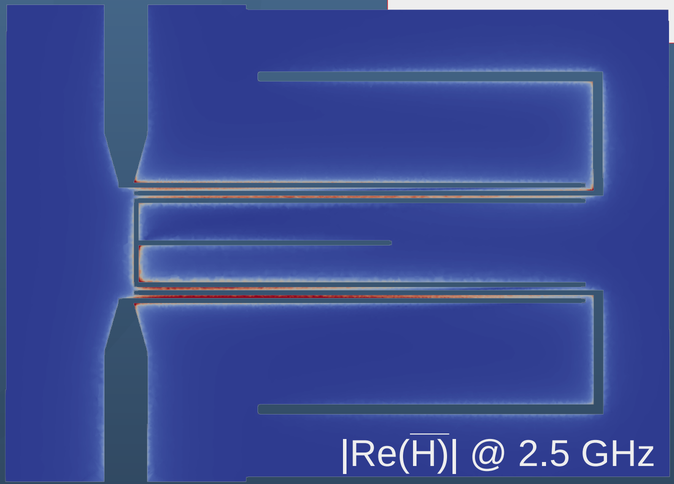

1 W.-C. Weng, "Design and Optimization of Compact Microstrip Wideband Bandpass Filter Using Taguchi's Method," *IEEE Open Access Journal*, vol. 10, 2022, pp. 107242-107249.

Regression Suites

- Automated
- With and without AMR
- OpenParEM2D
  - 27 test cases
    - Microstrip, stripline, coax, rectangular waveguide, loaded rectangular waveguide
  - 43,738 checks
- OpenParEM3D
  - 17 test cases
    - Microstrip, slotline, rectangular waveguide, loaded rectangular waveguide
    - Orientation variations (i.e. rotations in space)
  - 390 checks

Conclusions

- An effective 3D full-wave time-harmonic EM simulator for the calculation of S-parameters is outlined and demonstrated to produce high accuracy
- Lack of support for the gradient term $\nabla_t E_n$ on boundaries has two consequences
  - non-TE modes at ports require de-embedding (should be rare)
  - 2X run-time increase to separate forward and backward waves at the driving port due to the need to calculate $\overline{H}$
- To Do
  - Add impedance boundary condition for losses and antennas
  - Add PML for absorbing boundary condition at ports
  - Write documentation
  - Release

Thanks to LLNL’s Mark Stowell for many very helpful email exchanges.